

## Doubled Optical Path Length for Photonic Bandgap Fiber Gas Cell Using Micromirror

This content has been downloaded from IOPscience. Please scroll down to see the full text.

2011 Jpn. J. Appl. Phys. 50 06GM01

(<http://iopscience.iop.org/1347-4065/50/6S/06GM01>)

View [the table of contents for this issue](#), or go to the [journal homepage](#) for more

Download details:

IP Address: 130.237.165.40

This content was downloaded on 30/08/2015 at 09:53

Please note that [terms and conditions apply](#).

# Doubled Optical Path Length for Photonic Bandgap Fiber Gas Cell Using Micromirror

Xuefeng Li, Jinxing Liang<sup>1</sup>, Hiroshi Oigawa, and Toshitsugu Ueda

Graduate School of Information, Production and Systems, Waseda University, Kitakyushu 808-0135, Japan

<sup>1</sup>School of Instrument Science and Engineering, Southeast University, Nanjing 210096, China

Received September 18, 2010; revised January 3, 2011; accepted February 7, 2011; published online June 20, 2011

In this paper, we presented the double optical path length of a photonic bandgap fiber (PBGF) gas cell. The gas sensor sensitivity can be improved by a two fold lengthening of the optical length without changing the gas fluid. Furthermore, a high-reflection micromirror was included in the proposed double optical path length gas cell. A Cr/Au sputtering process was applied to fabricate the vertical micromirror using a single-mode fiber (SMF). A measurement system for low gas concentrations based on the micromirror has been implemented, and sensitivity was improved without increasing the response time. © 2011 The Japan Society of Applied Physics

## 1. Introduction

The photonic crystal fiber (PCF) is a new class of optical fiber based on the properties of photonic crystals.<sup>1-4</sup> Most PCFs are made of pure fused silica, and these fibers exhibit a host of novel and unusual transmission properties, which have prompted strong interest in recent years. There are several types of PCFs which differ in their structure and wave guiding mechanism. The photonic bandgap fiber (PBGF) has a hollow core surrounded by the periodic structure of the cladding, which confines light through bandgap effects. The Bragg fiber confines light in a relatively large-diameter hollow core formed by the concentric rings of multilayer films of different materials. The hole-assisted fiber has a solid core surrounded by an air-hole cladding structure, and guides light through a conventional higher index core modified by the presence of air-holes. Among these fibers, hollow core PBGFs are of particular interest for applications such as gas spectroscopy.<sup>5-12</sup> Typical PBGFs have unique structures, and more than 90% of optical power can be localized in the hollow core.<sup>13,14</sup> The hollow core can be filled with fluid, allowing light to interact with the fluid while it is being guided. Therefore, PBGFs are now widely used in highly sensitive gas sensors and other areas.

Strict control of the process atmosphere is required in the current lithography process. Because of lithography, the control of trace ammonia (NH<sub>3</sub>) gas has grown in importance, owing to its role as a source of foreign particles on the surface of the mask. To address the problems the low concentration of ammonia causes, it has been necessary to develop a real-time measurement technology. Ammonia molecules have a number of characteristic vibration absorption bands in the near-infrared (NIR) region.<sup>8,12,15</sup> The presence of NH<sub>3</sub> would result in a decrease in the output signal intensity when measured at 1531.7 nm because of the vibrational rotational absorption of the N-H molecules.<sup>16</sup>

The absorbance of NH<sub>3</sub> is generally in proportion to light path length in accordance with the Beer-Lambert law.<sup>8,9</sup> The detection of weak absorption will be greatly enhanced by increasing the overlap between the guided mode and the fluid. We have considered obtaining an absorption line with an adequate strength by using a longer PBGF. However, to assure fluid flow, a compromise between the strength of absorption and the optical path length is often needed. Many researchers have proposed some methods for increasing the optical length and reducing the gas flow length, mainly by drilling a hole on the PBGF or connecting

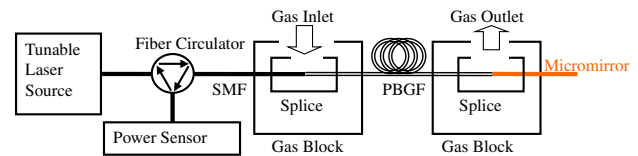


Fig. 1. (Color online) Experimental setup of doubled optical path length for photonic bandgap fiber gas cell using micromirror.

multiple PBGFs.<sup>9,10,17</sup> However, these methods have the problems of transmission loss and sensitivity to external vibration and heat, which limit the measurement sensitivity. Therefore, in order to improve the system sensitivity, we devised the double optical path length of a PBGF gas cell. A reflection mirror was arranged on one side of the PBGF to improve the gas sensor sensitivity by a two fold elongation of the optical length without changing the gas fluid (see Fig. 1). An advantage of this measurement system is the effective double optical path length of the gas sample. Therefore, the system sensitivity is improved without increasing the response time. The gap between the butt-coupled fibers is the most important parameter for maintaining good output coupling efficiency and allowing gas diffusion.<sup>16,18</sup> In general, a small gap means low loss. We drilled a micrometer-sized channel for gas flow through the fiber wall, by a focused ion beam (FIB) milling technique.<sup>16,19</sup> The achieved zero gap is expected to be effective for low-concentration gas measurement.

## 2. Measurement System

### 2.1 Production and evaluation of micromirror

In this study, the micromirror is made of a single-mode fiber (SMF) —28e from Corning®. A Cr/Au sputtering process is applied to fabricate vertical micromirrors for optical applications.<sup>20,21</sup> The fabrication process is as follows. (1) Remove the coating of the SMF. (2) Insert the fiber through the hole of the mechanical splice. (3) Cut the SMF to obtain a flat surface, using a fiber cutter. (4) Wash the SMF using ethanol followed by air. (5) Sputter Cr/Au metal films (50/200 nm). Figure 2 shows the image of the sputtering system and a scanning electron microscope (SEM) image of the micromirror with sputtered Cr/Au metal films for the SMF. Metal films may be damaged when the sputtered SMF is backed into the mechanical splice. In order to check the above hypothesis, we have prepared a series of 10 samples and inspected the cleaved facets with SEM. SEM images

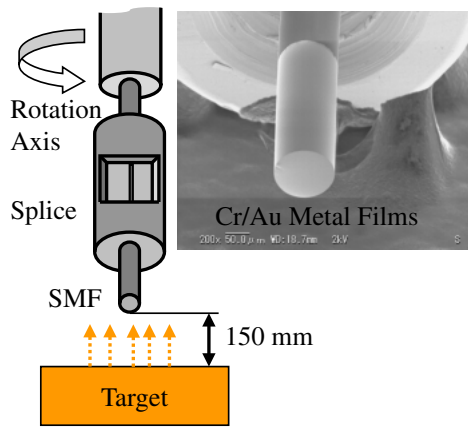


Fig. 2. (Color online) Scheme of sputtering system and SEM image of fabricated micromirror using Cr/Au sputtering process.

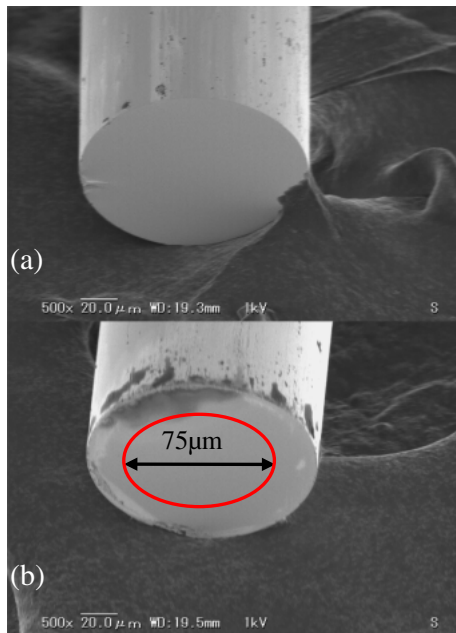


Fig. 3. (Color online) SEM images of metal films after micromirror was backed into mechanical splice. (a) Best sample of damaged metal films. (b) Worst sample of damaged metal films.

show the best and the worst of 10 samples in Figs. 3(a) and 3(b). Metal film was damaged at the periphery of the micromirror. The two most commonly employed PBGF structures have a core formed of either 7 or 19 omitted cells, and are called HC-1550-02 (HC02) and HC19-1550-01 (HC01). The measured core diameters are 10.9 and 20 μm, respectively. As shown in Fig. 3(b), even the worst sample had no damage in the central range of 75 μm diameter. This area is far greater than the mode field, and it can be utilized to act as a reflection micromirror.

To evaluate the reflection characteristics of the micromirror in the NIR range, we set up the experimental apparatus as shown in Fig. 4. The experimental system contains a Fabry–Perot (FP) tunable laser that is continuously swept from 1460 to 1640 nm at intervals of 0.1 pm wavelength and a power sensor with a power range of +10

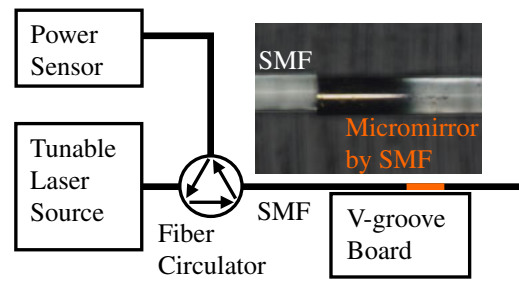


Fig. 4. (Color online) Measurement system for reflectance of micromirror.

to −100 dBm. A SMF is easily integrated with a micromirror using a V-shaped groove for light input and light output. The diameter of the SMF and the diameter of the micromirror are 8.2 and 75 μm, respectively. Therefore, the experimental apparatus can determine the reflectance of the micromirror. However, interference might make it difficult to evaluate the optical characteristics of the micromirror, owing to multiple reflections between the two flat surfaces of the micromirror and the corresponding end of the SMF. To suppress multiple reflections, zero gap between the two surfaces was calibrated on the microstage using an optical microscope.

Then the continuous-wave (CW) laser light was injected into a SMF through a fiber circulator, which was connected to a micromirror. The reflected light once again passed through the input SMF, and was received by a power sensor. An Au mirror deposited on a bare Si wafer has a known reflectance as high as 98% in the NIR range.<sup>21)</sup> The reflectance of the micromirror was measured in the NIR range from 1460 to 1640 nm, as shown in Fig. 5. The reflectance of the micromirror varied from 0.94 to 0.97, which almost corresponds to 0.98 of the theoretical value. Therefore, a high-reflection micromirror can be utilized in the proposed double optical path length gas cell.

### 2.2 Loss evaluation and discussion of optical access

The measurement system with a doubled optical path length incorporating a micromirror is shown in Fig. 1. The input end of the PBGF was spliced to a micromirror using a mechanical splice. In this study, the CW laser light was injected into a SMF through a fiber circulator, which was spliced to a PBGF. The reflected light once again was directed through the PBGF by the micromirror, and returned to the separated fiber circulator. Finally, it was received by the power sensor.

Since a small gap between two fibers corresponds to a low loss of splicing and can minimize the interference of multiple reflections between the two surfaces, the gap was adjusted to be zero.<sup>16,18)</sup> A micrometer-sized channel was opened by FIB milling at the lateral face to allow gas to flow in and out of the PBGF, as shown in Fig. 6(a). FIB milling is recognized as an indispensable tool in advanced microfabrication technologies.<sup>22–26)</sup> In this study, the PBGF was milled using Ga ions in the FIB 500 system from FEI Company. The FIB milling process was reported in our previous publication.<sup>16)</sup> To obtain a high milling rate, a high ion current of 6.4 nA is used, and a through-hole of 5 × 5 μm<sup>2</sup> was milled in 30 min. Figure 6(b) shows the connection between a PBGF (HC02) and a micromirror.

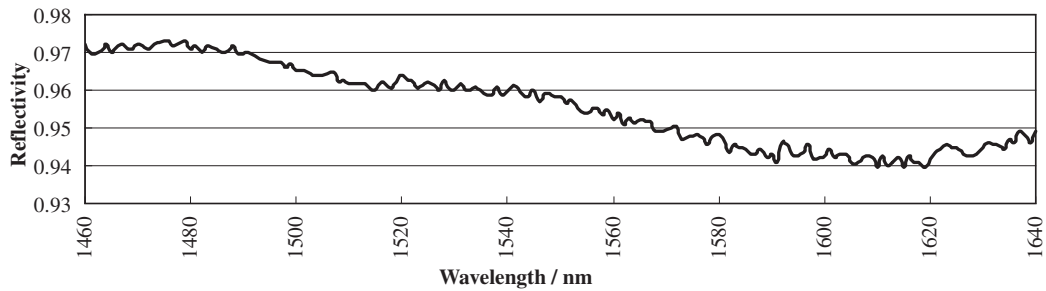


Fig. 5. Dependence of reflectance of the micromirror on wavelength.

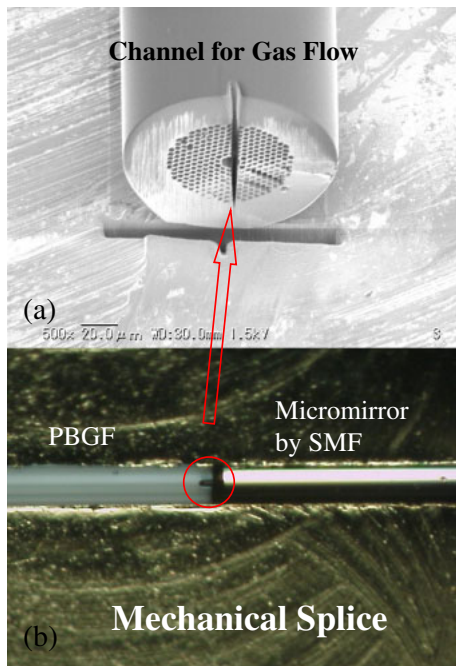


Fig. 6. (Color online) Micrometer-sized channel is opened at the lateral face of PBGF for gas flow. (a) SEM image of a through-hole of  $5 \times 5 \mu\text{m}^2$ . (b) Optical micrograph of connection of micromirror and PBGF (HC02).

A micrometer-sized channel for gas flow was opened. In the same manner as above, the other end of the PBGF is connected to a SMF, which is applied in gas concentration measurement.

For comparison, two types of measurement system are made with 1-m-long PBGFs. One type of experimental setup consists of a laser, a power sensor, a fiber circulator, a micromirror, and fibers, as shown in Fig. 1. It is called the micromirror reflection gas cell (MRGC) in this paper. The other one had no micromirror, and the output end of the PBGF was spliced to a SMF using mechanical splices, and the light at the output of the SMF was detected using a power sensor, as we reported previously.<sup>17)</sup> It is called the unidirectional gas cell (UGC). Losses of optical access are shown in Fig. 7. The solid black line indicates transmission loss from reflected light directed through the PBGF (HC01) by the micromirror. The solid gray line indicates the result of laser light passing unidirectionally through the PBGF (HC01) and spliced to the power sensor using a SMF. Transmission losses generally varied erratically from 10 to 20 dB. Transmission losses are mainly caused by the

mismatch of modes. Therefore, splice losses are small from the SMF to the PBGF, and most of the losses are generated from the PBGF to the SMF. The large variation is due to the effect of the wavelength on spatial power distribution.<sup>6,13,18)</sup> The dashed black line indicates transmission loss from MRGC using HC02. The dashed gray line indicates transmission loss from UGC using HC02. Transmission losses generally varied erratically from 5 to 10 dB owing to the mismatch of modes. The above-mentioned result clarified that losses of the micromirror are also very small.

### 3. Measurement of Ammonia Gas Concentration

In this study, using the proposed MRGC, the measurement system for low-concentration gas has been implemented. For comparison, both the MRGC and the UGC are made with 1-m-long PBGFs (HC01). The experimental setup is used to fill the PBGFs with gases and to perform absorption measurements. In the beginning, the gas absorption was measured using the UGC. The gas cell was evacuated with a rotary pump, and the appropriate gases ( $\text{N}_2$  or a mixture of both  $\text{NH}_3$  and  $\text{N}_2$ ) can be filled into the PBGF. Firstly, the PBGF was filled with  $\text{N}_2$  gas at 0.1 atm. The laser source was scanned from 1531.6 to 15731.8 nm with a reported spectral accuracy of 1 pm. Secondly, the PBGF was filled with 20 ppm  $\text{NH}_3$  gas at 0.1 atm. By the same method, the gas absorption was measured using the MRGC.

Figure 8 is the absorption spectrum of 20 ppm  $\text{NH}_3$  gas obtained by referencing the spectrum in  $\text{N}_2$  gas. The gray line shows 0.16 dB absorption using the UGC, and the black line shows an absorption about two times greater, 0.3 dB, using the MRGC. Therefore, the sensitivity was improved by the effective double optical path length of the gas sample. However, a slight deviation of the absorption peak was observed in the experiment. This variation is mainly caused by background noise and the wavelength accuracy of the tunable laser used. However, the relative wavelength accuracy of the tunable laser 81600B from Agilent,  $\pm 2.4$  pm (continuous sweep mode), is usually sufficient to identify molecular species.

### 4. Conclusions

In this study, we have proposed the double optical path length of the PBGF gas cell to improve the measurement system sensitivity. This is achieved by arranging a reflection mirror on one side of the PBGF. The reflected signal is received by the input SMF and it can be separated by a fiber circulator. The gas sensor sensitivity can be improved by a two fold elongation of the optical length without changing

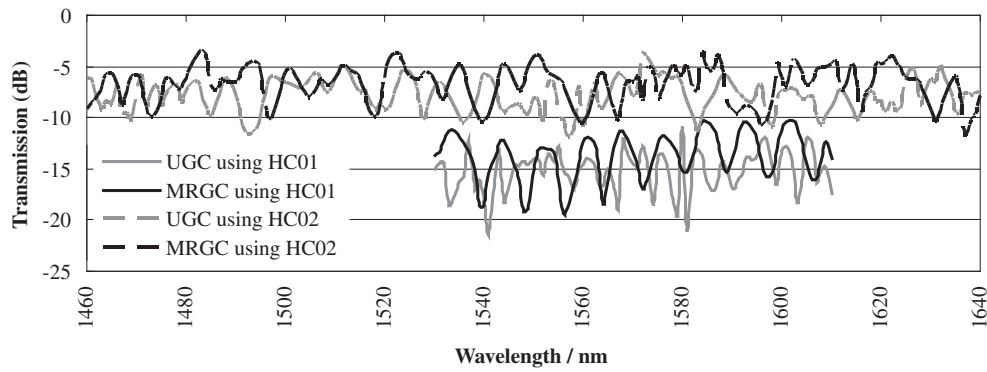


**Fig. 7.** Dependences of measurement systems on wavelength. Solid black line: transmission loss from MRGC using HC01. Solid gray line: transmission loss from UGC using HC01. Dashed black line: transmission loss from MRGC using HC02. Dashed gray line: transmission loss from UGC using HC02.

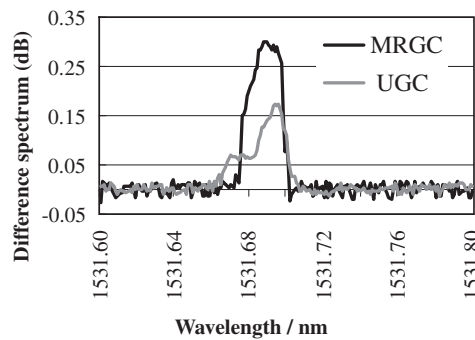


**Fig. 8.** Absorption spectra of 20 ppm NH<sub>3</sub>. Black line was obtained using MRGC with HC01, and gray line was obtained using UGC with HC01.

the gas fluid. Therefore, a high-reflection micromirror was incorporated into the proposed double optical path length gas cell. A Cr/Au sputtering process was applied to fabricate a vertical micromirror using the SMF. Reflectance of the micromirror almost corresponded to the theoretical value of 98% in the NIR range from 1460 to 1640 nm. Furthermore, the absorption spectrum of NH<sub>3</sub> gas was measured at a ppm-level concentration; it was demonstrated that the PBGF gas cell can be used in sensing low gas concentrations. Besides NH<sub>3</sub> gas, extensive research has been reported in recent years on measuring absorption spectra of gases such as CO, CO<sub>2</sub>, HCN, HF, H<sub>2</sub>S, NO, and hydrocarbons. Each PBGF is currently available for the wavelength range from 400 to 2550 nm. The broad wavelength region offers greater potential for gas sensing. This research result can contribute to the optical reflection in the gas measurement system using the PBGF cell.

**Acknowledgments**

This research is partly supported by Regional Innovation Cluster Program (Project number: 264084) which is organized by the Ministry of Education, Culture, Sports, Science and Technology, Japan.

- 1) P. St. J. Russell: *Science* **299** (2003) 358.
- 2) J. C. Knight: *Nature* **424** (2003) 847.
- 3) J. C. Knight: *J. Opt. Soc. Am. B* **24** (2007) 1661.
- 4) G. Humbert, J. C. Knight, G. Bouwmans, P. S. J. Russell, D. P. Williams, P. J. Roberts, and B. J. Mangan: *Opt. Express* **12** (2004) 1477.
- 5) F. Benabid, F. Couny, J. C. Knight, T. A. Birks, and P. St. J. Russell: *Nature* **434** (2005) 488.
- 6) R. Thapa, K. Knabe, K. L. Corwin, and B. R. Washburn: *Opt. Express* **14** (2006) 9576.
- 7) T. Ritari, J. Tuominen, H. Ludvigsen, J. C. Petersen, T. Sorensen, T. P. Hansen, and H. R. Simonsen: *Opt. Express* **12** (2004) 4080.
- 8) G. Pickrell, W. Peng, and A. Wang: *Opt. Lett.* **29** (2004) 1476.
- 9) Y. L. Hoo, W. Jin, C. Shi, H. L. Ho, D. N. Wang, and S. C. Ruan: *Appl. Opt.* **42** (2003) 3509.
- 10) J. P. Carvalho, H. Lehmann, H. Bartelt, F. Magalhães, R. Amezcua-Correa, J. L. Santos, J. Van Roosbroeck, F. M. Araújo, L. A. Ferreira, and J. C. Knight: *J. Sensors* **2009** (2009) 398403.
- 11) C. Young, S. Hartwig, A. Lambrecht, S. S. Kim, and B. Mizaikoff: Proc. IEEE Int. Conf. Sensors, 2007, p. 1345.
- 12) J. Pawlat, T. Sugiyama, X. Li, T. Matsuo, S. Ikezawa, and T. Ueda: *IEEE Trans. Sens. Micromach.* **128** (2008) 198.
- 13) M. N. Poletti, F. Poletti, A. Van Brakel, and D. J. Richardson: *Opt. Express* **16** (2008) 4337.
- 14) J. Tuominen, T. Ritari, H. Ludvigsen, and J. C. Petersen: *Opt. Commun.* **255** (2005) 272.
- 15) A. Schmohl, A. Miklós, and P. Hess: *Appl. Opt.* **41** (2002) 1815.
- 16) X. Li, J. Pawlat, J. Liang, G. Xu, and T. Ueda: *Jpn. J. Appl. Phys.* **48** (2009) 06FK05.
- 17) Y. Lai, K. Zhou, L. Zhang, and I. Bennion: *Opt. Lett.* **31** (2006) 2559.
- 18) P. Dominique, D. B. Philippe, and K. Nicolas: *Opt. Commun.* **110** (1994) 49.
- 19) C. Martelli, P. Olivero, J. Canning, N. Groothoff, B. Gibson, and S. Huntington: *Opt. Lett.* **32** (2007) 1575.
- 20) J. Liang, T. Matsuo, F. Kohsaka, X. Li, K. Kunitomo, and T. Ueda: *IEEE Trans. Sens. Micromach.* **128** (2008) 85.
- 21) K. W. Jo, S. S. Yun, N. Punithavelan, S. H. Jeong, S. K. Lee, and J. H. Lee: *J. Vac. Sci. Technol. B* **23** (2005) 2095.
- 22) C. Martelli, P. Olivero, J. Canning, N. Groothoff, B. Gibson, and S. Huntington: *Opt. Lett.* **32** (2007) 1575.
- 23) D. Iannuzzi, K. Heeck, M. Slaman, S. de Man, J. H. Rector, H. Schreuders, J. W. Berenschot, V. J. Gadgil, R. G. P. Sanders, M. C. Elwenspoek, and S. Deladi: *Meas. Sci. Technol.* **18** (2007) 3247.
- 24) B. C. Gibson, S. T. Huntington, S. Rubanov, P. Olivero, K. Digweed-Lyytikäinen, J. Canning, and J. Love: *Opt. Express* **13** (2005) 9023.
- 25) H. Kim, G. Hobler, A. Steiger, A. Lugstein, and E. Bertagnolli: *Opt. Express* **15** (2007) 9444.
- 26) Y. V. White, X. Li, Z. Sikorski, L. M. Davis, and W. Hofmeister: *Opt. Express* **16** (2008) 14411.